Heliyon 6 (2020) e03205

Contents lists available at ScienceDirect

Heliyon

journal homepage: www.cell.com/heliyon

Research article

Green corrosion inhibition and adsorption characteristics of *Luffa cylindrica* leaf extract on mild steel in hydrochloric acid environment

O.O. Ogunleye [a], A.O. Arinkoola [a,c,*], O.A. Eletta [b], O.O. Agbede [a], Y.A. Osho [a], A.F. Morakinyo [a], J.O. Hamed [d]

[a] *Department of Chemical Engineering, Ladoke Akintola University of Technology, Ogbomoso, Nigeria*
[b] *Department of Chemical Engineering, University of Ilorin, Ilorin, Nigeria*
[c] *Department of Petroleum Engineering, African University of Science and Technology (AUST), Abuja, Nigeria*
[d] *African Regional Centre for Space Science and Technology Education in English, Obafemi Awolowo University, Ile-Ife, Osun State, Nigeria*

ARTICLE INFO

Keywords:
Chemical engineering
Chemical synthesis
Materials characterization
Electrochemical engineering
Adsorption
Luffa cylindrica
Corrosion inhibition
Efficiency
Corrosion rate
Optimization
Isotherms
Thermodynamics
Kinetics

ABSTRACT

The corrosion inhibition of *Luffa cylindrica* Leaf Extract (LCLE) was investigated using gravimetric, depth of attack and surface analysis techniques. Effect of inhibitor concentrations (0.50–1.00 g/l), temperatures (30–60 °C) and immersion time (4–12 h) was studied on the Inhibition Efficiency (IE) of the extract on Mild Steel (MS) immersed in a 0.5 M HCl solution. The constituents of the proposed inhibitor were identified by using a GC-MS. The media solutions and adsorbed film on MS were characterized using FTIR Spectrophotometer. SEM microgram and surface tester were applied for studying surface morphology and depth of attack profile. The optimum IE of 87.89% was obtained. The LCLE adsorption on MS followed Langmuir isotherm and pseudo-second-order adsorption kinetics. Activation energy (28.71 kJ/mol), entropy (- 0.15 kJ/mol. K), average enthalpy (-28.00 kJ/mol) and Gibbs free energy (-11.43 kJ/mol) obtained at optimum condition indicate exothermic process and physical adsorption mechanism. The result obtained in this study compared well with many reported green inhibitors for MS corrosion.

1. Introduction

In many industrial operations, the addition of inhibitors to process fluids to minimize the rate of metal corrosion is very common. Chemicals are usually applied on metal surfaces as part of the final finishing procedures prior to plating, painting, or storage (Bentiss et al., 1999). According to Patricia et al. (2017), the chemicals are capable of removing scales, soil and light rust from the metal surfaces. Apart from this, they often contained about 1 % organic corrosion inhibitors by volume of the acid such as hydrochloric acid. Synthetic inhibitors have been widely applied to protect metal surfaces against corrosion (Zhang et al., 2012; Markhali et al., 2013). However, these inhibitors are toxic, expensive with environmental and safety issues. Alternative sources including natural products, extracts from plants, and other environmental benign organic sources have been widely reported (Sharma et al., 2015).

Many organic compounds have been tested for corrosion inhibition. The functionality of these compounds has been attributed to their electronegative functional groups and presence of π electrons in triple or conjugated double bonds. They also contain nitrogen, sulphur or oxygen atoms in their structures. Their mode of operation is by physical or chemical interactions between their molecules and the metal surfaces (Patricia et al., 2017). Several plant extracts including an extract from *Carica papaya, Rosmarinus Officinalis, Damsissa, Murrayakoenigii*, cashew, mango, *Uncaria gambir* and *Fiscusycomorus* had been investigated (Ebenso and Ekpe, 1996; Kliskic et al., 2000; Abdel-Graber et al., 2006; Ashish and Quraishi, 2010; Da Rocha et al., 2010; Hussain and Kassim, 2011; Ogwo et al., 2017; Ogunleye et al., 2018). According to Helen et al. (2014), these plants possess adequate cyclic organic phytochemicals, nitrogen, sulphur and oxygen atoms that are responsible for their inhibition properties. The large scale synthesis of various natural plant extract is faced with many challenges. The chief of which is the isolation of specific components of the plant extract with inhibitory characteristics. Nevertheless, many natural plant extracts have proven efficient as corrosion inhibitors (Ji et al., 2011; Kamal and Sethuraman, 2012; Yaro

* Corresponding author.
E-mail addresses: aoarinkoola@lautech.edu.ng, moranroolaakeem@yahoo.com (A.O. Arinkoola).

https://doi.org/10.1016/j.heliyon.2020.e03205
Received 6 November 2019; Received in revised form 25 December 2019; Accepted 9 January 2020
2405-8440/© 2020 Published by Elsevier Ltd. This is an open access article under the CC BY-NC-ND license (http://creativecommons.org/licenses/by-nc-nd/4.0/).

Figure 1. *Luffa cylindrica* plant.

Table 1. Process variable and their levels.

Factor	Name	Units	Low Actual	High Actual	Low Coded	High Coded
x_1	Concentration	g/l	0.1	0.5	-1	1
x_2	Temperature	K	303	363	-1	1
x_3	Time	h	4	12	-1	1

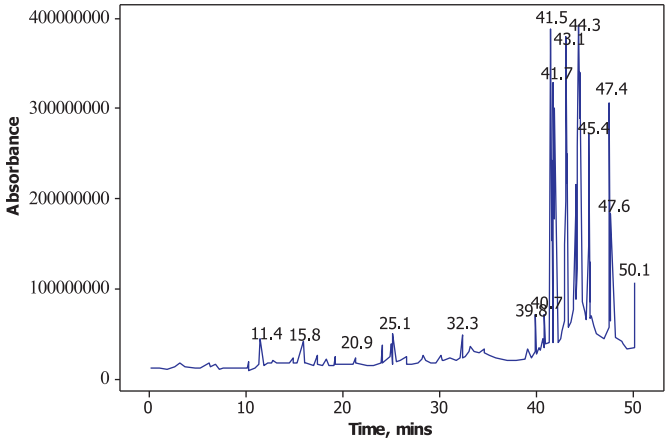

Figure 2. GC-MS chromatograph for LCLE.

et al., 2013). To gain insight on the working and applicability of natural extracts for commercial purposes, inhibition mechanism, kinetics and process thermodynamics was investigated on a pilot scale. The extract, after careful concentration under controlled temperature, may however, be added in the right mix to paints of organic solvent base for easy dissolution and dispersion.

Corrosion of metal takes place whenever there is an interaction of two different electrochemical reactions on the material surface. With detail knowledge of these electrochemical processes, potential theory is commonly applied for the prediction of corrosion rate. In many cases, these data are not available which limit the application of mixed potential theory with confidence. Laboratory measurements are therefore made and interpreted in terms of mixed potential theory such as polarization resistance, electrochemical impedance spectroscopy (EIS) and electrochemical noise (Markhali et al., 2013; Ostovari et al., 2009; Kliskic et al., 2000). These methods involve the use of advanced instruments with expert advice that are often not available to many researchers. Gravimetric-based method such as weight loss provides integrated mass

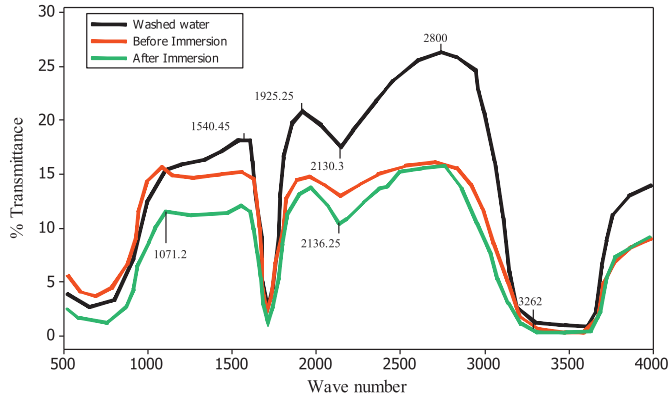

Figure 3. FTIR spectra for LCLE test solution (a) before immersion with IR peak ranged from 538.30 – 3594.05 cm-1 (b) after immersion with IR peak ranged from 602.64 – 3620.05 cm-1 and (c) washed coupon film with IR peak ranged from 588.13 – 3601.06 cm-1. These ranges suggest the presence and synergetic effect of O–H, C ≡ C stretch, C = O, Carboxyl and C–H groups in corrosion inhibition process.

loss information from corrosion that has occurred over some period of time. Because of simplicity and economic friendliness, gravimetric techniques are commonly used to measure general corrosion rate (Ogunleye et al., 2018). However, gravimetric-based techniques are unsuitable for continuous field monitoring of corrosion rates.

This present study deployed gravimetric and qualitative techniques to evaluate another eco-friendly material (LCLE), for use as an engineering inhibitor on MS submerged in a 0.5 M HCl solution. The optimum condition, the kinetics and thermodynamic parameters for maximum corrosion inhibition using LCLE were established.

2. Materials and equipment

The metal coupons utilized, chemical reagents, consumables and *Luffa cylindrical* plant were all sourced locally. Sensitive equipment such as soxhlet apparatus, evaporator, dryer, water bath, weighing balance and surface tester (PCE-RT 11) were employed for the test. Characterisation of materials and coupons was achieved by Gas Chromatography equipped with mass spectrophotometer (GC-MS; AGILENT 5789A), Fourier Transform Infra-Red (FTIR; BRUKER TENSOR 27) and Scanning Electron Microscopy (SEM; ZEISS equipment).

2.1. Extraction and analysis of Luffa cylindrica leaf extract

The *Luffa cylindrical* plant is a member of the cucurbitaceous family with smooth and rounded shaped fruits. It is called sponge gourd, vegetable sponge, bath sponge or dishcloth gourd (Velmurugan et al., 2011). Luffa plants grow by climbing on other physical solid materials. Typical leaves of a matured *Luffa cylindrical* plant is shown in Figure 1. The dried leaves of *Luffa cylindrica* plant was pulverized mechanically and screened to approximately 20 μm prior to extraction. Approximately 100 g of LCEC powder was soaked in 1000 ml of ethanol in a soxhlet extraction apparatus. The extract was then concentrated in a rotary evaporator and stored in an air-tight sterile container. The detail description of the extraction process is available elsewhere (Noyel et al., 2015). The constituent of the extract was identified using GC-MS. The dominant functional groups present in the extract before and after the corrosion study were identified using FT-IR.

2.2. Corrosion medium and coupon preparation

A 36 w/w % HCl (S.G = 1.18 gdm^{-3}) was serially diluted with distilled water to obtain desired 0.5 M HCl solution. Different concentrations (0.2–1.0 g/L) of LCLE were prepared for corrosion inhibition

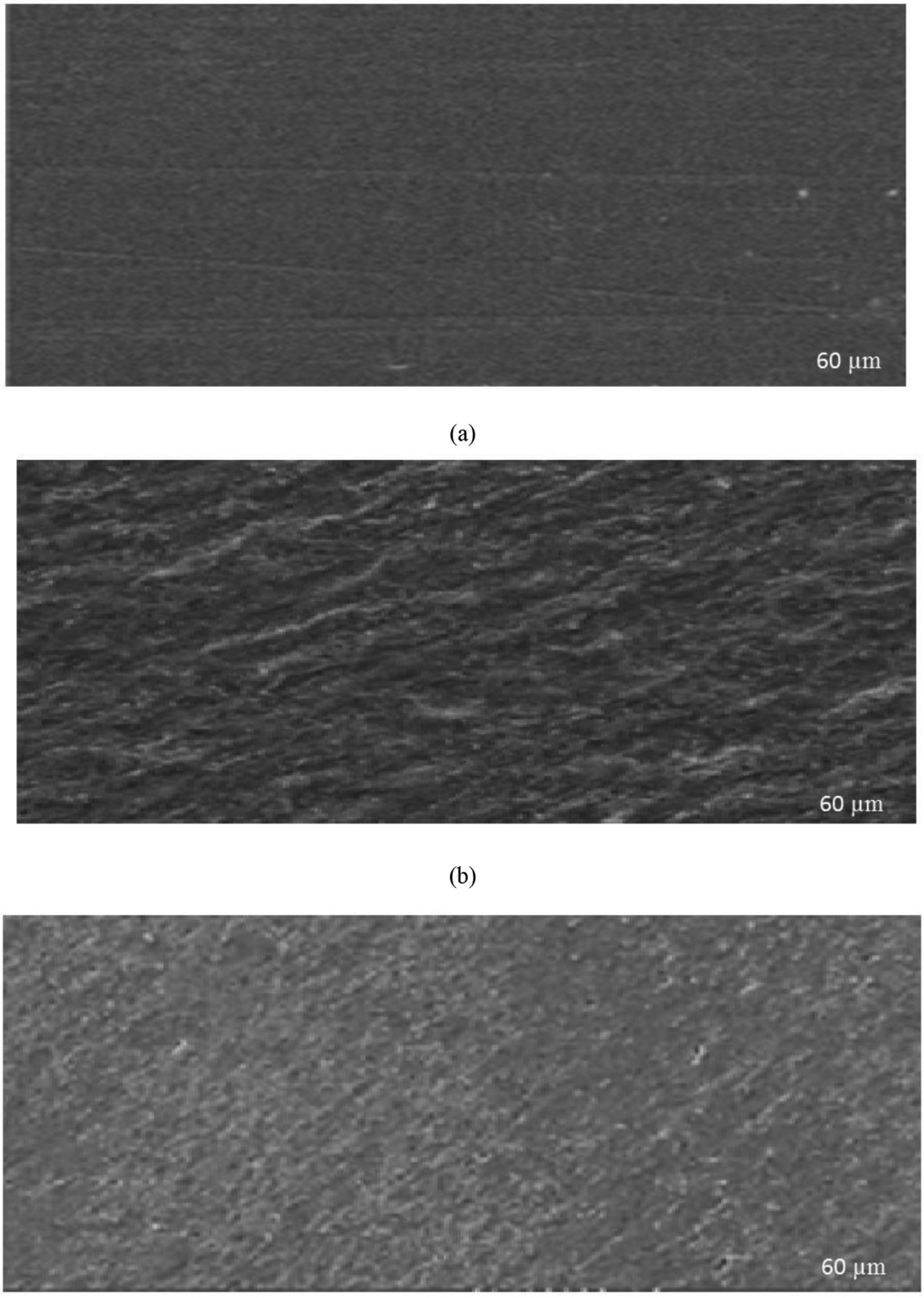

Figure 4. SEM images showing (a) unexposed polished MS (b) corroded surfaces of the exposed MS to 0.5 M HCl with no inhibitor (blank) and (c) the protected surfaces of the immersed MS in 0.5 m HCl +1 g/L of extract in 0.5 M HCl solution at test temperature of 60 °C after 12 h.

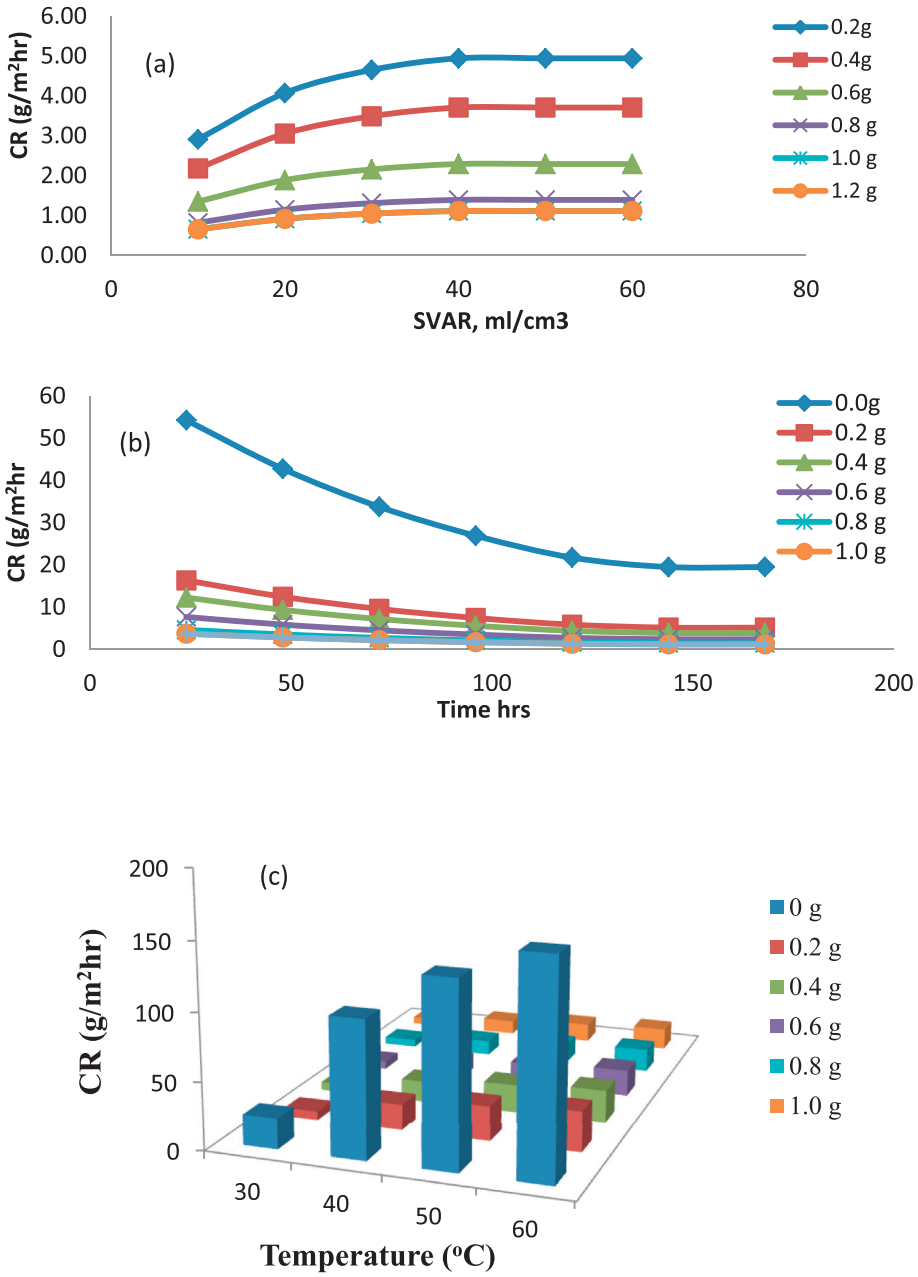

Figure 5. (a) Showing SVAR effects on CR. There is no more CR changes beyond SVAR of 40 ml/cm^3 for different inhibitor dosages (b) Showing CR versus immersion time for different inhibitor dosage. As immersion time increased, more protective film layer are formed on MS thereby slowed down the CR (c) Showing CR increases with temperature. More CR reduction observed with inhibited system compared with the control.

study following experimental design technique. The experiment without inhibitor (zero inhibitor) served as the control for all experiments. The corrosion media was sonicated and extract-HCl solution was homogenized using ultrasonic homogenizer (150VT) before the experiments in accordance with Singh et al. (2016).

Before the corrosion study, the coupon samples were carefully washed with a soft brush in high purity water, rinsed with acetone and then oven dried. This was as well done before measurements were done to minimize experimental error.

2.3. Weight loss method

A 3.5 cm × 3.0 cm x 0.3 cm MS coupons of composition 0.13, 0.18, 0.39, 0.40, 0.04 and 0.025, for C, Si, Mn, P, S, and Cu, respectively were used. The iron constituent makes up the composition to 100%. The corrosion measurements were made by recording the weight losses of MS coupons submerged in 100 ml corrosion medium in the presence and absence of inhibitor. A full factorial design was employed with all test carried out at 27 (±0.5) °C. The inhibitor concentrations were varied between 0 and 1.2 g/L at an interval of 0.2 g/L for periods of 24, 48, 72, 96, 144 and 168 h. After the experiment, equilibrium parameters were established and used for comprehensive batch corrosion studies. For each experiment, the coupon was weighed before the experiment (m_1) and after designated period, it was removed from test solution, washed, dried and then reweighed (m_2). The measurements were made in triplicate using OHAUS AX124 analytical balance of sensitivity ±0.0001 g. The mean values were noted and utilized for weight loss calculation using following equations:

Table 2. Surface maximum depth parameter at different temperature, concentration of *Luffa cylindrica* extract and time of immersion of MS in 0.5 MHCl.

Temp K	Inh. Conc. (g/L)	Time (hr)								
		4			8			12		
		R_Z (μm)	CR (μm/hr)	IE (%)	R_Z (μm)	CR (μm/hr)	IE (%)	R_Z (μm)	CR (μm/hr)	IE (%)
303	0.00	1.01	0.2525		1.84	0.2306		2.83	0.2360	-
	0.50	0.30	0.0752	70.24	0.55	0.0684	70.34	0.81	0.0676	71.34
	0.75	0.29	0.0714	71.73	0.51	0.0639	72.27	0.76	0.0630	73.32
	1.00	0.26	0.0661	73.83	0.47	0.0587	74.53	0.67	0.0562	76.20
	0.00	3.02	0.7558		5.35	0.6681		7.40	0.6163	-
318	0.50	0.68	0.1694	77.58	1.19	0.1487	77.75	1.56	0.1301	78.89
	0.75	0.61	0.1532	79.73	1.09	0.1361	79.64	1.43	0.1188	80.72
	1.00	0.53	0.1331	82.39	0.91	0.1138	82.97	1.21	0.1011	83.59
	0.00	5.93	1.4822		10.75	1.3443		15.97	1.3311	-
333	0.50	0.93	0.2314	84.38	1.57	0.1960	85.42	2.28	0.1899	85.73
	0.75	0.88	0.2193	85.21	1.48	0.1848	86.25	2.11	0.1760	86.78
	1.00	0.78	0.1955	86.81	1.36	0.1697	87.38	1.92	0.1600	87.98

R_z = maximum depth r = rate of attack IE = inhibition efficiency.

$$W = m_1 - m_2 \quad (1)$$

$$CR = \frac{W}{A \times t} \quad (2)$$

$$IE = \left[\frac{CR_0 - CR_I}{CR_O}\right] \times 100\% \quad (3)$$

$$\theta = \frac{IE}{100} \quad (4)$$

Where, CR is the corrosion rate of the coupon of surface area (A, cm^2) over time t. W is the weight loss. θ is the degree of inhibitor surface coverage and IE the inhibition efficiency.

2.4. Surface depth profiles

The surface morphologies of MS in the absence and presence of LCLE were studied to evaluate the nature and extent of surface roughness using SEM. To further determine the capability of LCLE as inhibitor, surface depth profiles were measured using surface tester (PCE-RT11). Its mode of operation is provided in Cai et al (2010). The peak height of irregularities (R_z) over a 2.5 mm sampling length was recorded. Similar to weight loss, the corrosion rate of MS in terms of R_z was estimated using the following equations:

$$\Delta Rz = Rz_f - Rz_i \quad (5)$$

$$CR_{Rz} = \frac{\Delta Rz}{l \times t} \quad (6)$$

$$IE_{Rz} = \left(\frac{r_{Rz}{}^O - r_{Rz}{}^I}{r_{Rz}{}^O}\right) \times 100 \quad (7)$$

2.5. Batch corrosion inhibition experiment

A set of experiments were carried out to study the effects of solution volume to coupon are ratio. This was done by varying the SVAR between 10 – 50 ml/cm^3 while temperature immersion time and inhibition

Table 3. Adsorption parameters for inhibition of MS in 0.5M HCl in the presence of LCLE at different temperature and time.

	4hr			8hr			12hr		
	303K	318K	333K	303K	318K	333K	303K	318K	333K
Freundlish isotherm									
slope	0.0398	0.0984	0.0766	0.0321	0.100	0.072	0.038	0.0923	0.0819
intercept	0.0626	0.0849	0.1336	0.0592	0.083	0.128	0.055	0.0776	0.1202
k_f	0.7352	0.1416	0.8658	0.7451	0.827	0.873	0.881	0.8364	0.7582
n	13.158	10.204	25.641	13.889	10.00	31.25	12.35	10.870	27.027
R^2	0.992	0.994	0.924	0.981	0.955	0.968	0.989	0.9450	0.9780
Langmuir isotherm									
slope	0.9234	0.9016	0.9602	0.928	0.900	0.968	0.918	0.9077	0.9622
intercept	0.1336	0.0849	0.0626	0.1278	0.083	0.059	0.120	0.0776	0.0550
K (l/g)	1.3602	1.2159	1.155	1.3421	1.209	1.146	1.319	1.1956	1.135
R^2	0.999	0.999	0.999	0.999	0.999	1	0.999	0.999	1
Temkin isotherm									
slope	0.0549	0.0783	0.034	0.0522	0.080	0.028	0.060	0.0755	0.0329
intercept	0.7352	0.8224	0.8658	0.745	0.827	0.873	0.758	0.8363	0.8809
B	0.0549	0.0783	0.034	0.0522	0.080	0.028	0.060	0.075	0.0329
K_T (mol/J)	45888	33767	81432	48261	33008	99952	41848	35253	84154
A_T	6.5E+05	3.6E+04	1.1E+11	1.6E+06	3.0E+04	4.8E+13	2.9E+05	7.0E+04	4.2E+11
R^2	0.999	0.993	0.922	0.983	0.951	0.967	0.99	0.941	0.978

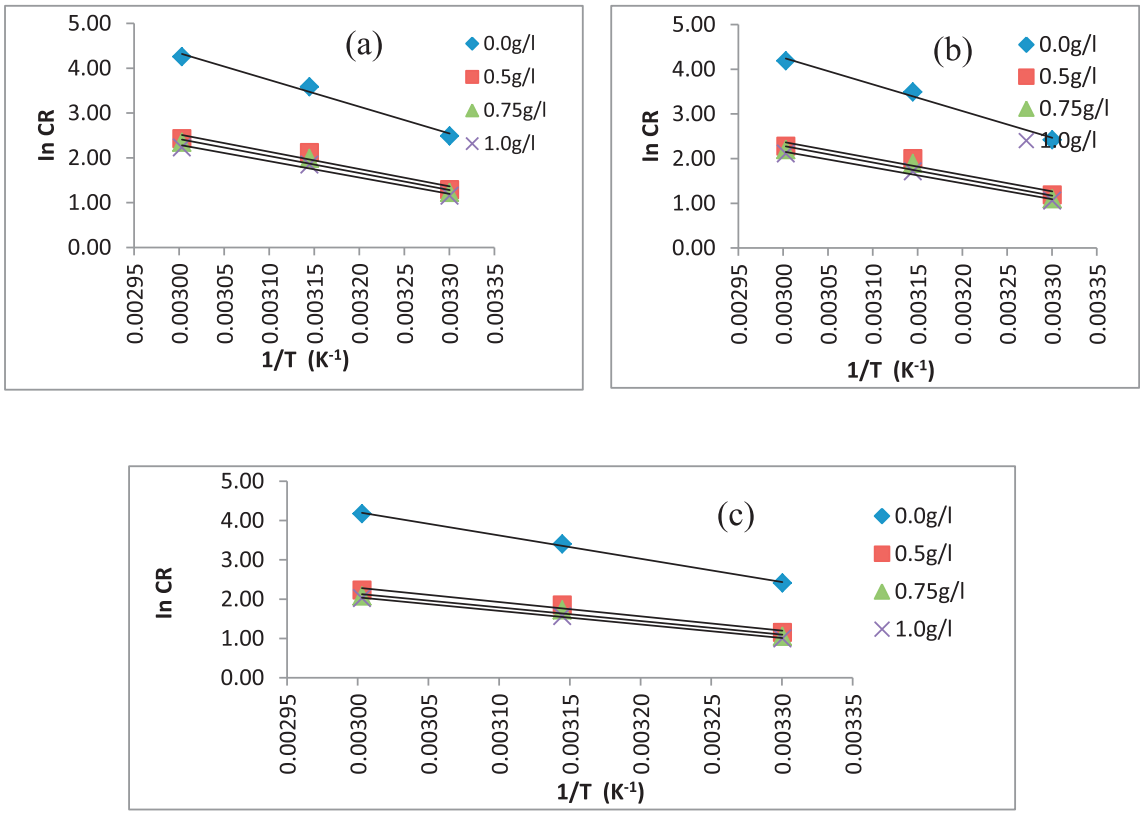

Figure 6. Arrhenius plot of ln CR vs 1/T for MS in the presence and absence of different concentrations of *Luffa cylindrica* extract after (a) 4 h (b) 8 h and (c) 12 h of immersion.

concentration were varied between (30–60 °C) (4–12 h) and (0.2–1.0 g/L), respectively. Another set of experiments were performed using 3-level factorial design to determine the optimal process parameters that maximize the inhibition of MS by LCLE in 0.5 M HCl solution. Here, the factors selected include concentration of inhibition, temperature and time of immersion. The SVAR was fixed at 40 ml/cm^3 for all experimental runs. Table 1 shows the summary statistics for the three selected factors.

For each experimental run, corrosion rate (CR) of the coupon of surface area (A, cm^2) over time t was calculated using both the weight loss (W) and depth profile techniques. The degree of inhibitor surface coverage (θ) and efficiency of inhibition (IE) were calculated.

2.6. Data analysis

Analysis of data and development of response surface models for CR and IE was achieved by Analysis of variance (ANOVA) and response surface methodology. The statistics considered are the F and p- values obtained at 95% confidence level. The goodness of models was ascertained using correlation coefficients (R^2 and adjusted R^2).

2.7. Adsorption isotherm

Adsorption isotherms explain the degree of interaction of molecules of various inhibitors with the metal surface (Ashish and Quraishi, 2010). Since corrosion inhibition using organic inhibitor occurs with the development of protective films caused by the adsorbed extract molecules on metal surfaces. Isotherm equations were used to confirm that the inhibition mechanism is truly adsorption. Also, to establish the closest equation that relates the concentration of inhibitors to the adsorbed concentration at saturation, the empirical equations such as exponential, hyperbolic, logarithmic and power are difficult to associate with the given mechanisms of the adsorption process. The Freundlich, Langmuir, and Temkin isotherms apart from their simplicity, are easy to apply to derive complete information from their parameters to characterize the corrosion inhibition system.

Customarily, adsorption isotherms are expressed in the form of Eq. (8) (Ameer et al., 2000).

$$f(\theta, x)\exp(-a\theta) = KC \tag{8}$$

The inhibition mechanism is invariably accompanied by the adsorption of molecules on the metal surface (Yaro et al., 2013; Fallavena et al., 2006). The fraction of the surface covered (θ)at any time was calculated using Eq. (4). For proper understanding of the mechanism involved for the case of LCLE and MS, the following isotherms were investigated:

2.7.1. Langmuir isotherm

The following equations describe the Langmuir adsorption isotherm. The 999 in Eq. (10) is the concentration of water (g/L) in solution. R is universal gas constant and T, temperature in (K).

$$\frac{C}{\theta} = \frac{1}{K_{Ads}} + C \tag{9}$$

$$K_{Ads} = \frac{1}{999}\exp\left(-\frac{\Delta G^{o}_{Ads}}{RT}\right) \tag{10}$$

2.7.2. Freundlich isotherm

Eq. (11) is a linearized form of Freundlich isotherm. A plot of Θ against C of data obtained at room temperature (303 K) was made on a log-log graph and isotherm parameters n and $K_{Ads,}$ were obtained as slope and intersect of the straight line. This was repeated for 318 and 333 K at (4, 8 and 12 h) using optimum concentration of LCLE.

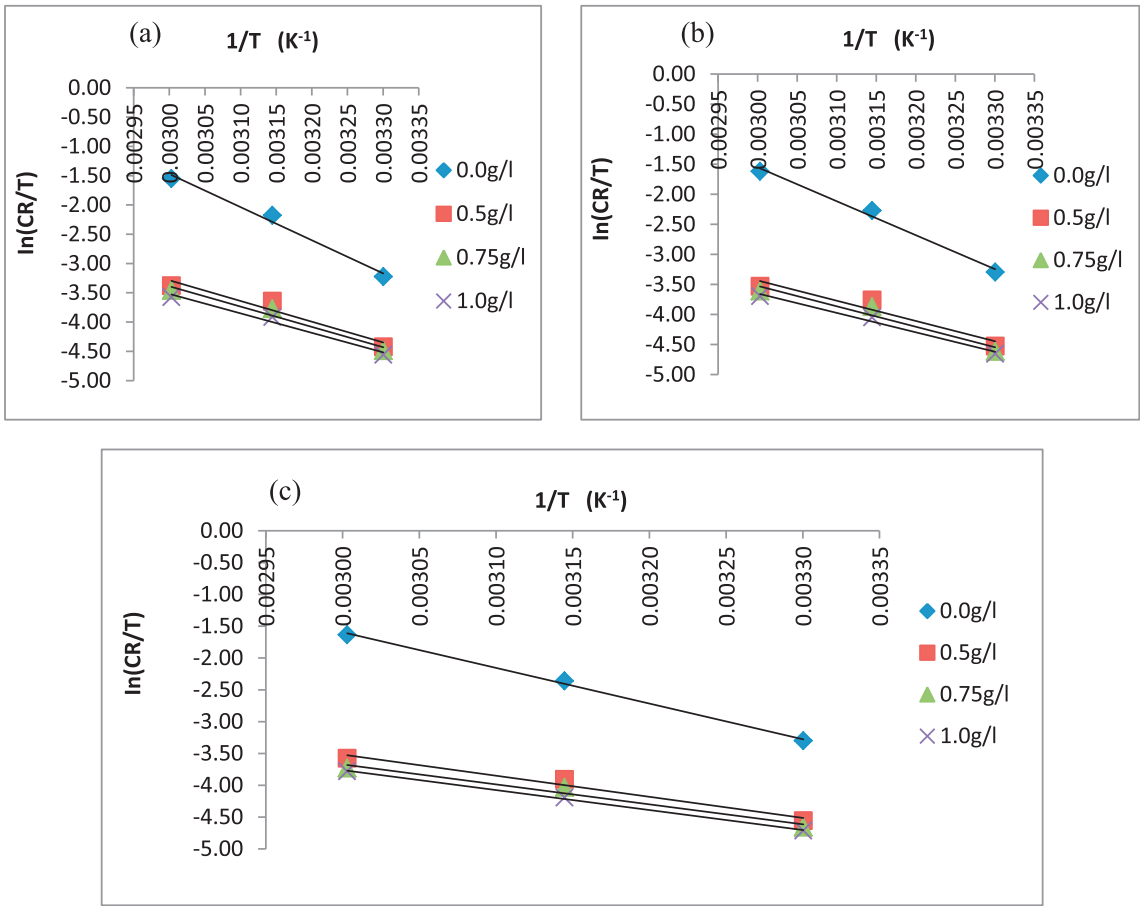

Figure 7. Transition state plot of In (CR/T) vs 1/T for MS in the presence and absence of different concentration of *Luffa cylindrica* extract after (a) 4 h (b) 8 h and (c) 12 h of immersion.

$$\log \theta = \log K_{Ads} + n \log C \tag{11}$$

2.7.3. Tempkin Isotherm

Eq. (12) related the degree of surface coverage (θ) and inhibition concentration (C). After linearization using logarithmic transformation, the constant K and parameter "a" were obtained for Tempkin Isotherm at various temperatures and time from Eq. (13). This was achieved by making a plot of θ against C.

$$e^{-2a\theta} = KC \tag{12}$$

$$\theta = \frac{-2.303 \log K}{2a} - \frac{-2.303 \log C}{2a} \tag{13}$$

Table 4. Thermodynamics parameters for inhibition of mild steel in 0.5M HCl in the presence of *Luffa cylindrica* extract at different temperature and time.

Time				
4hr				
IC g/l	ΔH KJ/mol	ΔS J/mol K	Ea KJ/mol	A
0.00	-47.001	-68.792	49.640	4.59E+09
0.50	-29.429	-136.577	32.068	1.32E+06
0.75	-28.897	-139.025	31.536	9.85E+05
1.00	-27.609	-143.983	30.248	5.42E+05
8hr				
0.00	-46.996	-69.449	49.635	4.24E+09
0.50	-28.048	-141.951	30.687	6.93E+05
0.75	-28.258	-142.068	30.897	6.83E+05
1.00	-26.919	-147.129	29.558	3.71E+05
12hr				
0.00	-46.612	-70.970	49.251	3.53E+09
0.50	-27.572	-144.081	30.211	5.36E+05
0.75	-26.085	-149.832	28.724	2.68E+05
1.00	-26.066	-150.632	28.705	2.44E+05

2.8. Corrosion inhibition kinetics

To determine optimum concentration of LCLE, it is necessary to explore dynamics of its inhibition. Corrosion rate in the presence of inhibitor and nature of its kinetics parameters dictate the selection of strategies suitable for effective corrosion control and management. The two kinetics models considered in this study are pseudo-first and second-order kinetic models represented by Eqs. (14) and (15), respectively.

$$\frac{d\theta}{dt} k_1(\theta_e - \theta_t) \tag{14}$$

$$\frac{d\theta}{dt} k_2(\theta_e - \theta_t)^2 \tag{15}$$

K_1 and K_2 (min^{-1}) are the rate constants obtained graphically following integration within necessary boundary limits. θ_e and θ_t represent degree of surface coverage at equilibrium and at a given time t.

2.9. Thermodynamic study

To determine the energy required, the heat involved and mechanism of corrosion in the presence or absence of inhibitor, the following ther-

Table 5. Free energy for inhibition of mild steel in 0.5M HCl in the presence of *Luffa cylindrica* extract at different temperature and time.

Temp (K)	Langmuir ΔG (KJ/mol)			Freundiich			Temkin		
	4hr	8hr	12hr	4hr	8hr	12hr	4hr	8hr	12hr
303	-10.88	-10.85	-10.81	-9.36	-9.39	-9.43	-37.90	-38.16	-38.03
318	-11.25	-11.20	-11.17	-10.00	-10.04	-10.08	-40.55	-40.40	-40.25
333	-11.56	-11.49	-11.45	-10.69	-10.75	-10.80	-40.73	-33.99	-40.30

Table 6. Kinetic parameters for inhibition of MS in 0.5M HCl in the presence of LCLE at different temperature.

	0.5 g/l			0.75 g/l			1.0 g/l		
	303K	318K	333K	303K	318K	333K	303K	318K	333K
Pseudo-first order									
K_1/hr	0.3385	0.3431	0.3155	0.4583	0.2994	0.3869	0.4076	0.3892	0.3731
θ_e	0.0893	0.1102	0.0525	0.2038	0.0555	0.1427	0.1645	0.1185	0.0733
$\theta_{e\ exp.}$	0.7167	0.7886	0.8585	0.7440	0.8082	0.8744	0.7576	0.8414	0.8804
R^2	0.933	0.829	0.999	0.921	0.724	0.895	0.839	0.870	0.896
Pseudo-second order order									
K_2/hr	6.2191	7.6716	5.5551	11.4931	5.3523	4.6493	6.0896	6.9618	4.5099
$\theta_{e\ value}$	0.7485	0.7994	0.8554	0.7468	0.8183	0.8749	0.7770	0.8251	0.9012
$\theta_{e\ exp.}$	0.7167	0.7886	0.8585	0.7440	0.8082	0.8744	0.7576	0.8414	0.8804
R^2	1	1	0.999	1	1	1	0.999	1	0.999

modynamics properties were determined experimentally: the activation energy (E_a), enthalpy (ΔHa°), and entropy (ΔSa°). By fitting experimental data to linearized form of Arrhenius and transition state equations, plots were particularly employed to determine these parameters using the Arrhenius Eq. (16) and the transition state Eq. (17):

$$C_R = A exp\left(-\frac{E_a}{RT}\right) \tag{16}$$

$$C_R = \frac{RT}{Nh} exp\left(\frac{\Delta S_o}{R}\right) exp\left(-\frac{\Delta H_o}{RT}\right) \tag{17}$$

$$\Delta G_{ads} = 2.303 \mathrm{RTlog}(55.5\mathrm{K}) \tag{18}$$

T represents the absolute temperature. A is the pre- exponential factor. N is Avogadro's number (6.02×10^{23} mol^{-1}), h is Plank's constant (6.63×10^{-34} J s^{-1}), K is equilibrium constant and the constant denoted by 55.5 denotes the molar heat of adsorption of water.

3. Results and discussion

3.1. Chemical constituents of LCLE

The GC-MS chromatograph showing the composition of LCLE is presented in Figure 2. The result shows that the principal active ingredient of LCLE is n-Hexadecanoic acid Dodecanoic acid with the highest peak value (22.18%) and retention time (39.894 min). The presence of carboxylic acid, hydroxyl and phenolic compounds suggested that the extract has a good corrosion inhibitory potential (Verma and Fahmida, 2016).

3.2. FTIR analysis of LCLE

The IR spectra of corrosion medium were captured before and after the corrosion. In addition, IR of the films adsorbed on the MS surface was taken by washing the coupon with distilled water. These results are presented as shown in Figure 3. The IR Peak observed in the test solution before immersion of mild steel ranged from 538.30 – 3594.05 cm^{-1} while the IR peak of test solution after immersion ranged from 602.64 – 3620.05 cm^{-1}. The coupon washed solution has IR Peak ranged from 588.13 – 3601.06 cm^{-1}. The dominant functional groups present in the three solutions are the wide broad band O–*H group* (3594.85–3262.40 cm^{-1}), C ≡ C stretch (2090.91cm^{-1}), C = O Carboxyl group (1638.14 cm^{-1}) and C–H bend alkyl group (605.80 cm^{-1}). Similar observations were also reported in the previous study (Okewale et al., 2016). According to Owate et al. (2014), the prevalence of carbonyl and double bond of carbon group in extracts of plants is an indication of corrosion inhibition characteristics.

The FTRIR analysis of the LCLE indicated the prevalence of oxygen- and nitrogen-containing compounds (hydroxy aromatic compound) such as flavonoids, tannins, pectins, and other organic compounds. The high value of corrosion inhibition efficiency recorded using LCLE in the 0.5 M HCl solution containing MS is attributed to the presence of hydroxy aromatic compounds. Tannins, for example, would form a passivating layer of tannates on the MS surface thereby slow down the corrosion rate. In addition, several OH groups in the extract could form strong links with other molecules which result in complexes formation with metals that causes blockage of micro anodes generated on the metal surfaces when in contact with electrolytes, and, hence, retard subsequent dissolution of the metal.

3.3. Surface morphology of test coupons

The surface characteristic of polished MS, the MS immersed in 0.5 M HCl without inhibitor (control) and MS immersed in 0.5 M HCl for 12 h in the presence of 1.0 g/L of LCLE at 60 °C are shown in Figure 4. The SEM image of MS coupon before immersion in the 0.5 M HCl solution containing no inhibitor (Figure 4b), revealed the presence of porous layers full of micro cracks. Consequently, the Chemicals can easily permeate the steel and can corrode the plate. However, in the presence of inhibitor (Figure 4c), the MS surface is notably improved considering its smoothness. It is also observed to be less porous with very minimal micro-cracks which are an indication of a reduction in corrosion rate. This improvement in surface morphology is due to the formation of a protective layer by LCLE on the surface of the metal. Therefore, using surface analysis it is shown that LCLE has a great tendency to adsorb to the MS surface and can be regarded as a good inhibitor for MS used in acidic medium.

Table 7. Responses of experimental design for inhibition process of MS in the presence of *Luffa cylindrica* extract in 0.5M HCl.

Std	Run	Factor 1	Factor 2	Factor 3	Response 1	Response 2
		X_1:inhi.Conc	X_2:Temp	X_3:time	Corrosion rate	Inhibition efficiency
		g/l	K	hr	g/m^2 hr	%
4	1	0.50	318	4	8.3238	76.92
18	2	1.00	333	8	8.2768	87.38
13	3	0.50	318	8	7.4133	77.42
15	4	1.00	318	8	5.5493	83.09
2	5	0.75	303	4	3.4062	71.73
28	6	0.75	318	8	6.6351	79.64
3	7	1.00	303	4	3.1755	73.64
10	8	0.50	303	8	3.2869	70.77
21	9	1.00	303	12	2.7185	75.68
22	10	0.50	318	12	6.3908	78.74
11	11	0.75	303	8	3.0055	73.27
14	12	0.75	318	8	6.6351	79.64
7	13	0.50	333	4	11.3705	84.38
19	14	0.50	303	12	3.1807	71.55
27	15	1.00	333	12	7.5813	87.98
16	16	0.50	333	8	9.7736	85.42
30	17	0.75	318	8	6.6351	79.64
9	18	1.00	333	4	9.3289	86.81
1	19	0.50	303	4	3.6382	69.80
31	20	0.75	318	8	6.6351	79.64
32	21	0.75	318	8	6.6351	79.64
6	22	1.00	318	4	6.3514	82.39
29	23	0.75	318	8	6.6351	79.64
23	24	0.75	318	12	5.6288	80.72
17	25	0.75	333	8	9.0117	86.81
5	26	0.75	318	4	7.3101	79.73
25	27	0.50	333	12	9.3299	85.73
8	28	0.75	333	4	10.4628	85.21
24	29	1.00	318	12	4.7898	84.06
26	30	0.75	333	12	7.9840	87.34
12	31	1.00	303	8	2.8853	74.34
20	32	0.75	303	12	2.8708	74.32

4. Sensitivity of CR to SVR, time and temperature

Corrosion rate was observed to vary with coupons SVR. This was investigated experimentally for varied range of SVR (10–50 ml/m^2), concentration (0.2–1.0 g/L) over corrosion period of 168 h at 27 °C. The optimum SVR was obtained at 40 ml/m^2, beyond which the CR remains relatively constant for irrespective of inhibition concentration used as shown in Figure 5a. The effect of time on corrosion rates for different inhibitor concentrations (0.2–1.2 g/L) at 27 °C for fixed SVR 40 ml/m^2 is shown in Figure 5b. The CR was observed to fall as immersion time and concentration of LCLE increases. However, a rapid reduction from 54.2 – 21.7 g/m^2.h of CR after 120 h of immersion was observed for control experiment with zero inhibitions. Upon addition of a mere 0.2 g/L LCLE, a tremendous reduction of CR from 24.16 – 4.38 g/m^2.h was observed over equal time interval between 0 and 120 h.

However, much more reduction of CR was observed after 120 h when inhibitor concentrations were increased above 0.2 g/L. In all the experiments, between 120 and 168 h, there was a gentle CR reduction from 21.7 to 19.5 g/m^2.h for control experiment and 4.36 to 2.4 g/m^2.h for the experiment with 0.2 g/L of LCLE. These observations agreed to Yaro et al. (2013) and Nathiya and Raj (2017).

Figure 5c show that CR of MS increases with temperature. The rate of corrosion, however, goes up more rapidly in the blank solution compared with inhibited systems. This can be explained by the increasing tendency of metals to dissociate quickly thereby causing partial desorption of the inhibitor from the metal surface as temperature increases. After 4 h of immersion, doubling the concentration of the extract from 0.5 to 1 g/l at 30, 45 and 60 °C, the corrosion rate decreases by 12.7, 23.7 and 18.0%, respectively. After 8 h at 0.5, 0.75 and 1.0 g/l of LCLE at 30 °C, the corrosion rate decreases by 9.7, 11.8 and 9.1% respectively as against 68.0, 67.4 and 66.0% when the temperature increases from 30 – 60 °C for 0.5 0.75 and 1.0 g/l of the LCLE respectively.

5. Corrosion depth measurements

Table 2 shows the measured CR and IE as a function of surface maximum depth of attack (Rz). It was observed at all temperature and immersion time that the pitting of the MS was reduced drastically as the concentration of LCLE increases compared to the control solution. This indicates that the corrosion of MS was effectively inhibited in the presence of the molecules of LCLE, and the etching of the MS surface is sensitive to the concentration of LCLE.

More so, it was evident that the IE of the LCLE increases as concentration increases. Inhibition efficiency recorded ranges from 70.24 to 88% at test conditions. Maximum IE (87.98%) was obtained with LCLE concentration 1.0 g/L for temperature up to 60 °C over 12 h of corrosion test.

6. Adsorption study

The result obtained from the various isotherms and thermodynamics was sufficient to explain the adsorption mechanism and inhibition potential of the LCLE molecules at the interface between the corrosion medium and MS. Table 3 shows the estimated parameters from the following isotherm graphs: Freundlich, Langmuir, and Temkin at different temperature and immersion time. The result revealed that the mechanism of LCLE adsorption on the surfaces of MS obeyed Langmuir isotherm at all studied temperature and time due to high values of R^2 and with the slope close to unity. This implies monolayer coverage and homogenous distribution of the LCLE molecules on the MS surface as assumed by Langmuir equation (Meroufel et al., 2013).

Also, the slope of the curve and its magnitude indicates existence and extent of electrostatic interaction of LCLE molecules with MS. Each of the molecules occupies one active site which agrees to Langmuir isotherm prediction of physisorption (Meroufel et al., 2013; Ogwo et al., 2017). Freundlich isotherm suggested a physical process as evident by the n values which ranged between 10 and 27.027. The value of n greater than unity at all temperature indicates adsorption of the extract on MS was based on heterogeneous interaction. However, the correlation coefficient R^2 values obtained at different temperatures are quite low when

Table 8. Analysis of variance for corrosion rate and inhibition of MS in 0.5 M HCl.

	MODEL	Sum of	df	Mean	F-value	p-value
IE (%)	Quadratic	910.984	9	101.220	236.909	<0.0001
				R^2 = 0.989	Adj. R^2 = 0.986	Pred. R^2 = 0.9768
CR (g/m2 hr)	Quadratic	189.376	9	21.042	373.884	<0.0001
				R^2 = 0.993	Adj. R^2 = 0.991	Pred. R^2 = 0.9836

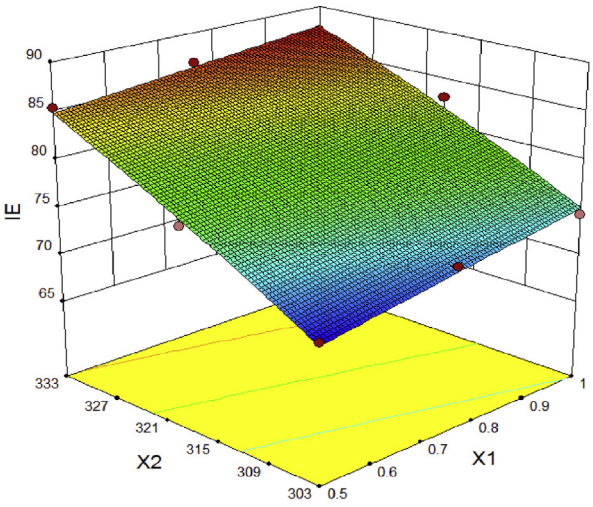

(a) Temperature (X_2) and inhibitor concentration (X_1) on IE

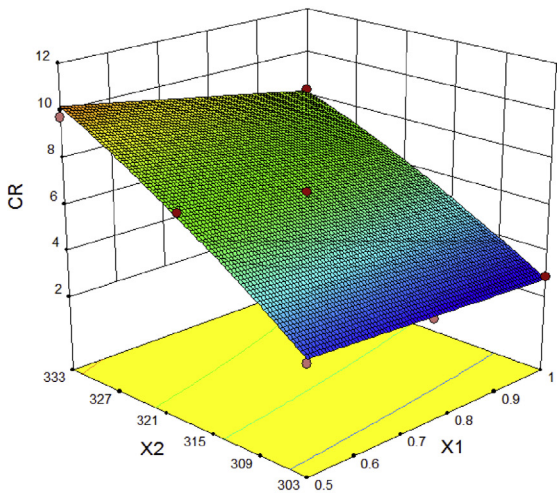

(b) Temperature (X_2) and inhibitor concentration (X_1) on CR

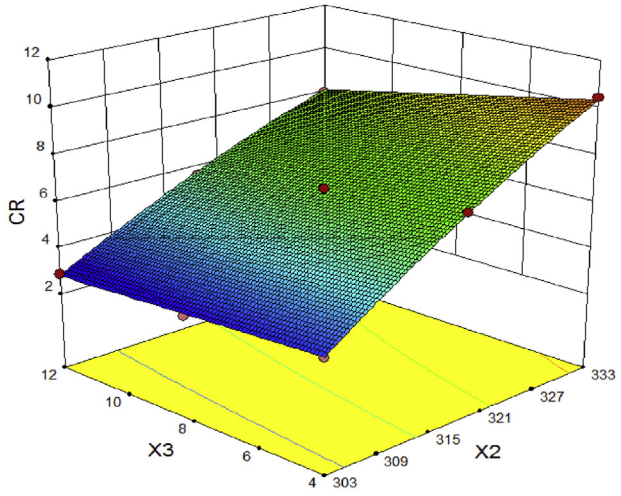

(c) Temperature (X_2) and time (X_3) on CR

Figure 8. Factor interaction as affects the IE of LCLE for the corrosion of MS in 0.5M HCl (a) The effect of temperature and inhibitor concentration. As inhibition concentration increased from minimum to maximum concentration, the IE increases with temperature (b) Effect of time and inhibition concentration. For any fixed amount of LCLE in the system, the IE increases with time but high for higher concentration of inhibitor (c) Effect of temperature and time. Temperature exhibited greater effects with maximum IE at higher temperature.

compared with that from Langmuir isotherm. Similar observation was made for the Temkin isotherm. The Langmuir constant shows a higher constant value of 1.3602 L/g at 303K which indicates that the extract is strongly adhered on the MS surface at 303 K and 12 h (Aprael et al., 2013).

7. Thermodynamics studies

Figure 6 shows the Arrhenius plot used for estimating the E_a after 4, 8 and 12 h of immersion of MS in 0.5 M HCl in the presence and absence of different LCLE concentrations. The values of E_a estimated ranges from 28.7 - 32.07 kJ/mol for all concentrations of LCLE. According to Eddy and Ebenso (2008), Rani and selvaraj, (2010), the values of Ea< 80 kJ/mol indicate physical adsorption while E_a > 80 kJ/mol indicates chemical adsorption. Thus, the interaction of LCLE molecules that led to adsorption on MS surface followed physical mechanism.

Figure 7 shows the transition state plot for control and inhibited system after 4, 8 and 12 h of corrosion process while Table 4 shows parameters estimated at different temperature and time. The enthalpy changes (ΔH_{Ads}) at different concentrations of LCLE and immersion time

Table 9. Comparison of inhibition efficiency of LCLE with other natural inhibitors on MS.

Natural Products	Percentage Inhibition	References
Pectin from citrus peels	94.20%	Fiori-Bimbi et al. (2015)
Punica granatum peel extract	92.40%	Behpour et al. (2012)
Longan seed and peel extracts	92.93%	Liao et al. (2017)
Griffonia simplicifolia extract	91.73%	Ituen et al. (2017)
Water Melon rind extract	83.35%	Odewunmi et al. (2015)
Justicia gendarussa extract	93.00%	Satapathy et al. (2009)
Murraya Koenigii extract	84.60%	Sharmila et al. (2010)
MIPE	95.75%	Ogunleye et al. (2018)
LCLE	87.89%	This study

were negative which indicated exothermic (Iloamaeke et al., 2015). The change in enthalpy obtained ranged between -26.066 and -29.429 kJ/mol across test temperature (303–333 K) and indicated a physisorption mechanism (Meroufel et al., 2013). The negative values of entropy ΔS_a revealed a decrease in disorderliness. The adsorption free energy (ΔG_a) ranges between -11.56 and -11.45 kJ/mol at 333 K as shown in Table 5. Negative ΔG_a explains the feasibility and spontaneous nature of the adsorption. The values obtained at 333 K shows good interaction between its molecules and the MS surface which confirms that the LCLE is strongly adsorbed on MS (Dakeshwar and Fahmida, 2016). According to Dakeshwar and Fahmida, (2016), ΔGa values of -20 kJ/mol or less negative are associated with physisorption while those of with more negative than -40 kJ/mol are associated with chemical adsorption. Thus, the adsorption of LCLE molecules on the surface of MS is said to follow physical adsorption mechanism.

8. Kinetics and optimization studies

Table 6 shows the result obtained after fitting the experimental data; concentration (0.5–1.0 g/l), temperatures (303–333 K) and time (0–12 h) to the two kinetic models selected for this study. With correlation coefficient (R-square values) criteria, it was observed that the corrosion of MS in the presence of LCLE obeys the pseudo-second-order kinetics with R-square value ranged between 0.9999 – 1.

The 32 experiments performed for optimization of IE and CR are presented in Table 7 which was analysed using analysis of variance**.** The ANOVA confirmed the suitability of quadratic models for the CR and IE with F-value of 373.88 and 236.909, respectively. The p – values recorded were less than 0.0001 for both CR and IE and attest to the reliability of the analysis with 95 percent confidence level. The final equations in terms of actual factors are presented in Eqs. (19) and (20). The values of correlation, adjusted and predicted R-squares (Table 8) show that the model equations are predictive and can reliably useful for sampling data within the experimental range of parameters. Figure 8 shows factor interaction as it affects the IE and CR of MS in 0.5M HCl.

$$\begin{aligned} CR\left(g/m^2h\right) = & -257.333 + 25.365 * Inh.Conc + 1.360 * Temp \\ & + 1.848 * Time - 0.088 * Inh.Conc * Temp \\ & + 0.055 * Inh.Conc * Time - 0.0067 * Temp * Time \\ & - 0.332 * Inh.Con^2 - 0.00163 * Temp^2 + 0.00368 * Time^2 \end{aligned} \quad (19)$$

$$\begin{aligned} IE(\%) = & -356.937 + 40.2195 * Inh.Conc + 2.1577 * Temp \\ & + 0.7882 * Time - 0.10889 * Inh.Conc * Temp \\ & - 0.0033 * Inh.Conc * Time - 0.0024 * Temp * Time \\ & + 1.4211 * Inh.Con^2 - 0.00252 * Temp^2 + 0.01211 * Time^2 \end{aligned} \quad (20)$$

Eqs. (20) and (21) represent objective functions. CR was minimized while IE was maximized subjected to the constraints shown in Table 1. The maximum IE of 88.35% was obtained at 0.99 g/L of extract concentration, temperature of 332.81K and immersion time of 10.15 h using numerical optimization technique. The minimum CR of 7.63 g/m^{2}h was obtained at optimum condition. The validity of these numerical values was established experimentally and the value of 87.89 ± 0.325 percent and 7.91 ± 0.0282 g/m^{2}h for IE and CR respectively attested to the consistency and representativeness of the model for prediction purposes. Table 9 shows the result of comparative study of IE recorded from this study with other known green inhibitors. It is evident that the result obtained in this study compared well with some green inhibitors that have been applied to MS.

9. Conclusion

The capacity of LCLE as a green corrosion inhibitor has been assessed in this research by using the weight loss, depth of attack and surface analyses. The extract showed good inhibition characteristic for mild steel in 0.5 M HCl solution due to the presence of tannins, phenol, flavonoids, and alkanol groups according to the GC - MS and FTIR analyses. The inhibition efficiency improved with increasing inhibitor concentrations and decreased with increasing temperature. The result obtained using weight loss and depth of attack methods are consistent. At a concentration of 1.0 g/L, the extract proved to be an excellent inhibitor with an efficiency of 87.89 ±0.325% at 332.81K after 10 h. FTIR spectra revealed the presence of functional groups containing hetero-atoms. The SEM analysis showed that the inhibitor adsorption forms a protective film on the MS surface. The adsorption of extract film was found to follow Langmuir isotherm and pseudo-second-order kinetics. The values of the activation energy, enthalpy, Gibbs free energy and parameters estimated from the isotherm models suggested that the adsorption mechanism of LCLE on the MS is physisorption and exothermic.

Declarations

Author contribution statement

Ogunleye, O.O.: Conceived and designed the experiments; Wrote the paper.

Arinkoola, A.O. & Agbede, O.O.: Analyzed and interpreted the data; Wrote the paper.

Eletta O.A. & Hamed J.O.: Contributed reagents, materials, analysis tools or data; Wrote the paper.

Osho, Y.A. & Morakinyo A.F.: Performed the experiments; Analyzed and interpreted the data.

Funding statement

This work was supported by the Tertiary Education Trust Fund (TETFUND), Ladoke Akintola University of Technology, Ogbomoso, Nigeria.

Competing interest statement

The authors declare no conflict of interest.

Additional information

No additional information is available for this paper.

Acknowledgements

The authors acknowledge Chemical Engineering laboratories of both LAUTECH and UNILORIN for technical support.

References

Abdel-Graber, A.M., Abd-El-Nabey, B.A., Sidahmed, I.M., El-Zayady, A.M., Saadawy, M., 2006. Effect of temperature on inhibitive action of Damsissa extract on the corrosion of steel in acidic media. Corros. Sci. 62 (4), 239–299.

Ameer, M.A., Khamis, E., Al-Senani, G., 2000. Adsorption studies of the effect of thiosemicarbazides on the corrosion of steel in phosphoric acid. Adsorpt. Sci. Technol. 18 (3), 177–194.

Aprael, S.Y., Anees, A.K., Rafal, K.W., 2013. Apricot juice as green corrosion inhibitor of mild steel in phosphoric acid. Alexandria Eng. J. 52, 129–135.

Ashish, K.S., Quraishi, M.A., 2010. Effect of cefazolin on the corrosion of mild steel in HCl solution. Corros. Sci. 52, 152–160.

Behpour, M., Ghoreishi, S.M., Khayatkashani, M., Soltani, N., 2012. Green approach to corrosion inhibition of mild steel in two acidic solutions by the extract of *Punica granatum* peel and main constituents. Mater. Chem. Phys. 131 (3), 621–633.

Bentiss, F., Lagrenee, M., Traisnel, M., Hornez, J.C., 1999. The corrosion inhibition of mild steel in acidic media by a new triazole derivative. Corros. Sci. 41, 789–803.

Cai, B., Lui, Y., Tian, X., Wang, F., Li, H., Ji, R., 2010. An experimental study of crevice behaviour of 316L stainless steel in artificial seawater. Corros. Sci. 52, 3235–3242.

Dakeshwar, K.V., Fahmida, K., 2016. Green approach to corrosion inhibition of mild steel in hydrochloric acid medium using extract of spirogyra algae. Green Chem. Lett. Rev. 9 (1), 52–60.

Da Rocha, J.C., Da Cunha, P., Gomes, J.A., Elia, E.D., 2010. Corrosion inhibition of carbon steel in hydrochloric acid solution by fruit peel aqueous extract. Corros. Sci. 52 (7), 2341–2348.

Ebenso, E.E., Ekpe, U.J., 1996. Kinetic study of corrosion and corrosion inhibition of mild steel in sulphuric acid using *Carica papaya* leave extract. West Afr. J. Biol. Appl. Chem. 41, 21–27.

Eddy, N.O., Ebenso, E.E., 2008. Adsorption and inhibitive properties of ethanol extracts of *Musa sapientum* peels as a green corrosion inhibitor for mild steel in H_2SO_4. Afr. J. Pure Appl. Chem. 2 (6), 046–054.

Fallavena, T., Antonow, M., Goncalves, R.S., 2006. Caffeine as nontoxic corrosion inhibitor for copper in aqueous solutions of potassium nitrate. Appl. Surf. Sci. 253, 566–571.

Fiori-Bimbi, M.V., Alvarez, P.E., Vaca, H., Gervasi, C.A., 2015. Corrosion inhibition of mild steel in HCl solution by pectin. Corros. Sci. 92, 192–199.

Helen, L.Y., Rahim, A.A., Saad, B., Saleh, M.I., Bothi, R.P., 2014. Aquilaria crassna leaves extracts – a green corrosion inhibitor for mild steel in 1.0 M HCl medium. Int. J. Electrochem. Sci. 9, 830–846.

Hussain, H.M., Kassim, J.M., 2011. The corrosion inhibition and adsorption behaviour of Uncaria gambir extract on mild steel in 1M HCl. Int. J. Mater. Chem. Phys. 12 (5), 46-468.

Iloamaeke, I.M., Egwuatu, C.I., Umeobika, U.C., Edike, H., 2015. Corrosion inhibition and adsorption studies of ethanol extract of *Senna alata* for mild steel in 2.0M H_2SO_4 solution. Int. J. Mater. Chem. Phys. 1 (3), 295–299.

Ituen, E., Akaranta, O., James, A., Sun, S., 2017. Green and sustainable local biomaterials for oilfield chemicals: Griffonia simplicifolia extract as steel corrosion inhibitor in hydrochloric acid. Sustain. Mater. Technol. 11, 12–18.

Ji, G., Shukla, S.K., Dwivedi, P., Sundaram, S., Prakash, R., 2011. Inhibitive effect of argimone mexicana plant extract on acid corrosion of mild steel. Ind. Eng. Chem. Res. 50, 11954–11959.

Kamal, C., Sethuraman, M.G., 2012. Caulerpin-A bis-indole alkaloid as a green inhibitor for the corrosion of mild steel in 1 M HCl solution from the marine alga caulerpa racemose. Ind. Eng. Chem. Res. 51, 10399–10407.

Kliskic, M., Radosevic, J., Gudic, S., Katalinic, V., 2000. Aqueous extract of osmarinus officianliis L. As inhibitor of Al-Mg alloy corrosion in chloride solution. J. Appl. Electrochem. 30 (7), 823–830.

Liao, L.L., Mo, S., Luo, H.Q., Li, N.B., 2017. Longan seed and peel as environmentally friendly corrosion inhibitor for mild steel in acid solution: experimental and theoretical studies. J. Colloid Interface Sci. 499, 110–119.

Markhali, B.P., Naderi, R., Mahdavian, M., Sayebani, M., Arman, S.Y., 2013. Electrochemical impedance spectroscopy and electrochemical noise measurements as tools to evaluate corrosion inhibition of azole compounds on stainless steel in acidic media. Corros. Sci. 75, 269–279.

Meroufel, B., Benali, O., Benyahia, M., Benmoussa, Y., Zenasni, M.A., 2013. Adsorptive removal of anionic dye from aqueous solutions by algerian kaolin: characteristics, isotherm, kinetic and thermodynamic studies. J. Mater. Environ. Sci. 3 (4), 482–491.

Nathiya, R.S., Raj, V., 2017. Evaluation of *Dryopteris cochleata* leaf extracts as green inhibitor for corrosion of aluminium in 1 M H_2SO_4. Egypt J. Pet. 26 (2), 313–323.

Noyel, V.S., Rohith, P., Manivannan, R., 2015. *Psidium guajara* Leaf extract as green corrosion inhibitor for mild steel in phosphoric acid. Int. J. Electrochem. Sci. 10, 2220–2238.

Odewunmi, N.A., Umoren, S.A., Gasem, Z.M., 2015. Utilization of watermelon rind extract as a green corrosion inhibitor for mild steel in acidic media. J. Ind. Eng. Chem. 25, 239–247.

Ogunleye, O.O., Eletta, O.A., Arinkoola, A.O., Agbede, O.O., 2018. Gravimetric and quantitative surface morphological studies of *Mangifera indica* peel extract as a corrosion inhibitor for mild steel in 1 M HCl solution. Asia Pac. J. Chem. Eng., e2257

Ogwo, K.D., Osuwa, J.C., Udoinyang, I.E., Nnanna, L.A., 2017. Corrosion inhibition of mild steel and aluminium in 1 M hydrochloric acid by leaves extracts of Ficus sycomorus. Phys. Sci. Int. J. 14 (3), 1–10.

Okewale, A.O., Omoruwou, F., Ojaigho, R., 2016. Alternative energy production for evironmental sustainability. Br. J. Renew. Energy 1 (2), 18–22.

Ostovari, A., Hoseinieh, S.M., Peikari, M., Shadizadeh, S.R., Hashemi, S.J., 2009. Corrosion inhibition of mild steel in 1 M HCl solution by *henna* extract: a comparative study of the inhibition by *henna* and its constituents (lawsone, gallic acid, a-D-glucose and tannic acid). Corros. Sci. 51, 1935–1949.

Owate, I.O., Nwadiuko, O.C., Dike, I.I., Isu, J.O., Nnanna, L.A., 2014. Inhibition of mild steel corrosion by *Aspilia africana* in acidic solution. Am. J. Mater. Sci. 4 (3), 144–149.

Patricia, E.A., Fiori-Bimbi, M.V., Adriana, N., Silvia, A.B., Claudio, A.G., 2017. Rollinia occidentalis extract as green corrosion inhibitor for carbon steel in HCl solution. J. Ind. Eng. Chem.

Rani, P.D., selvaraj, S., 2010. *Emblica officinalis* (AMILA) leaves extract as corrosion inhibitor for copper and its alloy (Cu- 272N) in natural sea water. Archived Appl. Sci. Res. 2 (6), 140–150.

Satapathy, A.K., Gunasekaran, G., Sahoo, S.C., Amit, K., Rodrigues, P.V., 2009. Corrosion inhibition by *Justicia gendarussa* plant extract in hydrochloric acid solution. Corros. Sci. 51 (12), 2848–2856.

Sharmila, A., Prema, A.A., Sahayaraj, P.A., 2010. Influence of *Murraya koenigii* (curry leaves) extract on the corrosion inhibition of carbon steel in HCl solution. Rasayan J. Chem. 3 (1), 74–81.

Sharma, S.K., Anjali, P., Obot, I.B., 2015. Potential of *Azadirachta indica* as a green corrosion inhibitor against mild steel, aluminum, and tin: a review. J. Anal. Sci. Technol. 6, 26–42.

Singh, P., Srivastava, V., Quraishi, M.A., 2016. Novel quinoline derivatives as green corrosion inhibitors for mild steel in acidic medium: electrochemical, SEM, AFM, and XPS studies. J. Mol. Liq. 216, 164–173.

Velmurugan, V., Shiny, G., Surya Surekha, P., 2011. Phytochemical and biological screening of *Luffa cylindrica* linn. Fruit. Int. J. PharmTech Res. 3 (3), 1582–1585.

Verma, D.K., Fahmida, K., 2016. Green approach to corrosion inhibition of mild steel in hydrochloric acid medium using extract of spirogyra algae. Green Chem. Lett. Rev. 9 (1), 52–60.

Yaro, A.S., Khadom, A.A., Wael, R.K., 2013. Apricot juice as green corrosion inhibitor of mild steel in phosphoric acid. Alexandria Eng. J. 52, 129–135.

Zhang, G.A., Zeng, Y., Guo, X.P., Jiang, F., Shi, D.Y., Chen, Z.Y., 2012. Electrochemical corrosion behavior of carbon steel under dynamic high pressure H_2S/CO_2 environment. Corros. Sci. 65, 37–47.